SRIM as a Computational Tool to Study Energy Required during Prostate Cancer Treatment

Karan Giri, Aarati Khatiwada and Pooja Bista

Journal of Nepal Physical Society
Volume 8, No 1, 2022
(Special Issue: ICFP 2022)
ISSN: 2392-473X (Print), 2738-9537 (Online)

JNPS, **8** (1), 48-54 (2022)
DOI: http://doi.org/10.3126/jnphyssoc.v8i1.48285

Published by: Nepal Physical Society
P.O. Box: 2934
Tri-Chandra Campus
Kathmandu, Nepal
Email: nps.editor@gmail.com

ICFP 2022
ISSN:2392-473X (Print)
2738-9537 (Online)

Research Article ©Nepal Physical Society
DOI:http://doi.org/10.3126/jnphyssoc.v8i1.48285

SRIM as a Computational Tool to Study Energy Required During Prostate Cancer Treatment

Karan Giri,[1, a)] Aarati Khatiwada,[2] and Pooja Bista[2]

[1)]*Tri-Chandra Multiple Campus, Tribhuvan University*
[2)]*Sainik Awasiya Mahavidyalaya, Tribhuvan University*

[a)]*karangiri575@gmail.com*

Abstract. Proton beam therapy is a promising technique to cure various types of cancer diseases in the human body. Employing this technique, the prostate cancer cells are damaged primarily leaving the surrounding cells unaffected. Initially, the position of the prostate cancer is determined then the energy required to damage cancerous cells is calculated computationally. The energy loss to the damaged cells and other layers of the human body via which the proton beam travels is calculated separately with high accuracy. It is found that 65 MeV energy of proton beam when interacts with various layers, particularly with cancerous cells, the maximum energy is imparted to these cancerous cells to destroy them effectively. TRIM data shows that 99.96% of the energy of proton is lost in the process of ionization by ion and 0.02% in ionization by recoils and only 0.01% energy is lost by production of phonon by ion and 0.02% by recoils. 65 MeV of the energy deposited on various layers viz. skin, connective tissue, soft muscles and prostate are approximately 0.384 MeV (i.e. 0.595%), 6.585 MeV (i.e. 10.20%), 14.654 MeV (22.71%), and 42.896 MeV (66.49%) respectively with the calculation error 0.74%. Ion range and lateral distribution calculation enable us to visualize the overall picture of the process of the simulation. SRIM data illustrates that more than 99% of the energy of the proton is lost during the ionization process while phonon production is almost negligible. The energy of proton beam deposited on various layers viz. skin, connective tissue, soft muscles and prostate cancerous cells among them the prostate cells receive the maximum energy. This technique not only cures prostate cancer effectively but also ensures that it has no side effects and the surrounding tissues or cells remain unaffected.

Received: 11 March, 2022; **Revised**: 14 April, 2022; **Accepted**: 2 May, 2022

Keywords: Proton beam therapy, Radiation therapy, Prostate cancer, Stopping power

INTRODUCTION

Background

Proton beam therapy (PBT) is a kind of particle therapy technique that employs a proton beam to irradiate affected tissue/s in the human body. Owing to the excellent physical properties and dosimetric parameters, PBT has been used in a variety of cancers treatments [1]. Wilson proposed PBT for the first time in 1946. Researchers at the Lawrence-Berkeley National Laboratory published the first PBT case series after a 12-year wait. Several other proton treatment facilities emerged throughout the world during the next few decades, and PBT has now been utilized in the clinical environment for more than 60 years, treating tens of thousands of patients with various forms of cancer. The appropriate application of PBT has led to fewer adverse effects and higher therapeutic efficacy compared with conventional RT using X-ray beams. Thus, facilities for PBT are being built worldwide, despite the requirement for costly equipment [2, 3, 4]. Over the past decades, with an increasing number of PBT applications worldwide, the number of new programs under development is growing. The reason for this is that the proton dose distribution that may be achieved is generally superior to the dose distribution of conventional photon radiation therapy (PRT). PBT may improve the survival rate of patients by improving the local tumor treatment rate, while reducing injury to normal organs, resulting in fewer radiation-induced adverse effects. The clinical benefits of PBT have been established in terms of less side effects when compared to photon treatment. However, the use of PBT is controversial due to the high treatment costs associated with proton facility development and maintenance. When compared to photon treatment, however,

the higher cost may be justified because of the improved quality of life and lower expenditures associated with advanced illness care. More clinical research is needed to determine whether PBT will benefit patients. More research and discussion are needed to address the use of PBT in various malignancies, as well as how to maintain patients' quality of life while achieving a high cure rate [5]. In recent decades, as the number of PBT applications around the world has grown, so has the number of new programs in development. Because the proton dosage distribution that may be achieved is generally superior to the photon dose distribution, this is the rationale. PBT has the potential to improve patient survival rates by enhancing local tumor treatment rates while reducing damage to normal organs, resulting in fewer radiation-induced adverse effects. Compared to typical photon RT, heavier subatomic particles are able to convey their energy more accurately to the tumor, with less scattering to adjacent tissues. PBT is associated with obvious benefits, such as reducing the volume of irradiated normal tissue, improving the conformability and the quality of the target area.

Data showed 11.5% i.e. 45 of proton patients experienced a grade three or higher side effect. In the photon group, 27.6% i.e. 301 experienced a grade three or higher side-effect. A weighted analysis of both patient groups, which controlled for other factors that may have led to differences between the patient groups, found that the relative risk of a severe toxicity was two-thirds lower for proton patients compared to photon patients [2]. Importantly, overall survival and disease-free survival were similar between the two groups, suggesting that the reduction in toxicity seen with proton therapy did not come at the cost effectiveness. Further studies and discussions are required to make proton therapy cost effective and to address its use in several types of cancer, and for maintaining the quality of life of patients while achieving a high cure rate. The aim of this paper is to report the characteristics and current development in PBT.

Prostate Cancer

The prostate gland (found only in men) is located near the urethra: just below the bladder and in front of the rectum, and performs many functions including producing seminal fluid (used to nourish and transport sperm), regulating and controlling urine flow by contracting and releasing muscle fibers and depends on adequate levels of testosterone to function properly. In young men, the prostate is around the size of a walnut, and it grows larger as the man gets older. In prostate cancer, abnormal cells proliferate and form a tumor on the prostate. It is caused by alterations in the DNA of a normal prostate cell at its most basic level and can spread to other regions of the body if it is not treated, including the bones, lymph nodes, and, in certain cases, the rectum, bladder, and lower ureters [6, 7, 8].

METHODS AND SIMULATION DETAIL

Most aspects of the energy loss of ions in matter are calculated using SRIM. It performs quick calculations producing tables of stopping powers, range and straggling distributions for any ion at any energy in any elemental target. More elaborate calculations include targets with complex multi-layer configurations. NIST [9, 10] produces the Nation's Standard Reference Data (SRD). These data are assessed by experts and are trustworthy such that people can use the data with confidence and base significant decisions on the data. The SRD program includes the Journal of Physical and Chemical Reference Data. The PSTAR program is used calculate stopping power and range tables for protons in various materials for energies in the range from 0.001 MeV to 100 Mev. The specification

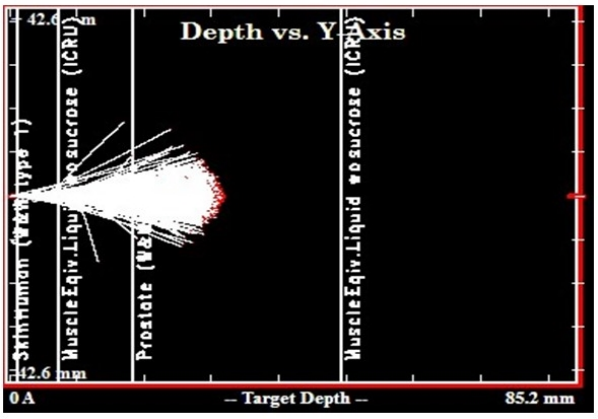

FIGURE 1. Image depicting SRIM simulation result.

of energy for the required range is done by performing simulation on water phantoms. SRIM stopping and range tables are employed for water to determine the energy required to reach the desired depth for effective irradiation. We are interested to irradiate the tumor at prostate gland and study the physics of dose deposition. The prostate gland is at the depth of 31 mm from the skin and assuming tumor is located somewhere between prostate gland we have selected the energy value 65 MeV for proton beam for which the range projected is 35.15 mm. The image of the simulation which is obtained after 99999 protons (this number can also be reduced) hitting the target is depicted in FIGURE 1 in which white dots represent the path of protons while red dots represent recoiling atoms. The range radial and projected range and their straggle are also depicted.

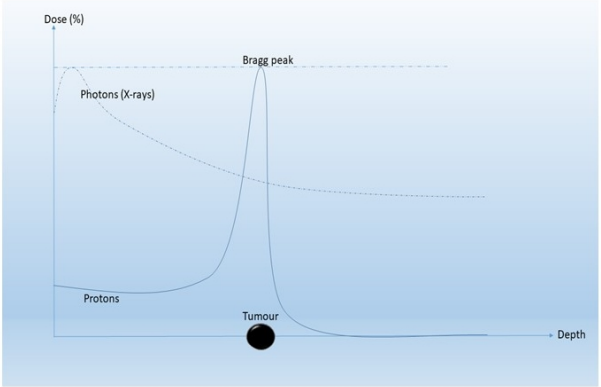

FIGURE 2. A comparison between proton beam therapy and conventional radiation therapy depicts why former one is better choice for caner treatment.

THEORY

In PBT technique, a particle accelerator targets a tumor with a beam of protons. The energetic proton beam is allowed to impinge the affected part and is slowed down as a result of interactions with the target. This leads to a sharp rise in energy deposition at the desired area or volume i.e. a high dose can be delivered to the specific area, followed by no further dose delivery. This is termed the Bragg peak and such specific property provides superior dosimetric advantages over electrons or photons [11, 12]. Therefore, rather than traversing the target, protons are stopped at an energy-dependent depth in the target and have no exit dose, which completely spares the downstream normal tissue. Unlike photons, which deposit most of their energy at their entrance into the body, protons deposit their maximum energy at the Bragg peak. Before this peak, the deposited dose is about 30% of the Bragg peak maximal dose. Following that, the deposited dose drops to almost nil, yielding a nearly undetectable exit dose. The integral dose with proton therapy is approximately 60% lower than any photon-beam technique [13, 14]. Thus, proton therapy delivers radiation to tumors and areas in very close proximity, decreasing integral radiation dose to normal tissues and theoretically avoiding collateral damage. The sketch of dose delivery to the cancerous tissue by proton beam and X-ray beam is depicted in FIGURE 2.

The crucial things for the efficient treatment of tumors are: how the protons interact with the biological matter and how much energy is deposited into the tissues which provide the information about a dose received during therapy. The experiments on human tissues are complicated so a simple model or theoretical program is to be created which can be employed to calculate the dose distributions in that matter. This can be done by a computer program called the stopping and range of ions in matter (SRIM).

Stopping Power and Range

When proton beam passes through the various layers of human body it interacts with the atoms results in different layers [15, 16, 17]. There are mainly two kinds of interactions: the electronic and nuclear interaction. The former one is when energized beam of protons pass near orbiting electrons, the positive charge of the protons attracts the negatively charged electrons, pulling them out of their orbits, also called ionization. And the latter one is when proton interacts with atom losing its energy in the form of atomic vibration i.e. phonon production. Both interactions are responsible for the stopping of radiation in matter. Hence, total stopping power (S) is the sum of electronic stopping power and the nuclear stopping power. While passing through matter, both charged and uncharged particles lose energy. The stopping power of radiation depends on the type and energy of the radiation as well as the qualities of the material through which it passes. The Bloch function is used to express the stopping power S of a material that is quantitatively equivalent to the loss of energy (E) per unit path length (x) [15, 18].

$$S = -\frac{dE}{dx}$$

$$S = \left(\frac{e^2}{4\pi\varepsilon_0}\right)^2 \frac{4\pi N_A Z\rho}{mc^2\beta^2 A}\left[ln(\frac{2mc^2\beta^2}{I}) - ln(1-\beta^2) - \beta^2\right] \quad (1)$$

The quantity $-\frac{dE}{dx}$ is the negative of energy gradient, also known as the stopping power (the negative sign signifies the energy loss), $\beta = v/c$,is ratio of velocity of the particle to the speed of light,$\varepsilon_0, e, m, N_A, Z, A, \rho$,and I are vacuum permittivity, electronic charge, rest mass, Avogadro number, atomic number, atomic mass number, density, and excitation potential respectively. The distance "x" is not always expressed in meters, but often in units of mass per square meter. This latter parameter comes from multiplying the length parameter by the density of the material. This is a more convenient and useful unit of material thickness as far as experimentalists are concerned. The force usually increases toward the end of the range and reaches a maximum, the Bragg peak, shortly before the energy drops to zero. The curve that describes the force as a function of the material depth is called the Bragg curve [19]. This is of great practical importance for radiation therapy. In passing through matter, charged particles ionize and thus lose energy in many steps, until their energy is (almost) zero. The distance to this point is called the range of the particle. The range depends upon the type of particle, on its initial energy, and on the material through which it passes. The mean range can be cal-

TABLE I. Detail of the various layers of the human body through which proton beam travells.

Layer	Layer Name	Layer Width (mm)	Layer Density(gcm
1	Skin	1.2	1.09
2	Connective Tissue	5	0.92
3	Soft Muscles	4.8	1.07
4	Prostate	20	1.04

culated by integrating the reciprocal stopping power over energy [20]:

range,

$$R(E) = \int_0^{E'} (\frac{dE'}{dx})^{-1} dE \approx \sum_0^E (\frac{dE}{dx})^{-1} \Delta E \qquad (2)$$

where E is the ion's initial kinetic energy. The summation denotes that the continuous transport is approximated by calculations of discrete steps. In fact, as discussed above, this equation truly gives the path length, which is an excellent approximation of range in the most clinical situation. Radiotherapy, one of the three pillars in today's cancer therapy is preferable and is better than both chemotherapy and surgery. A simple principle common in them is to destroy cancerous tissue and spare healthy ones. Cancer is one of the prime causes of death therefore the development of radiation therapy (RT) and medical imaging is a necessity. During this process, medical physicists have been facing numerous challenges. One of the major challenges for them is the improvement and transfer of technology into medicine. In RT, this is achieved by deposition of radiation energy (RE) locally as a result there is no correct repair of the DNA and the cell cannot reproduce itself. This local deposition of RE normalized by the irradiated mass is dose.

RESULTS AND DISCUSSION

Target Discription

The anatomy of prostate gland of adult human is simulated and the trajectory which the beam of proton will follow during the therapy is specified. Various entrance layers to reach the tumor site and their corresponding properties viz. width, density and composition is given in TABLE I. These layers are selected from the compound dictionary of SRIM.

Calculation of Energy

The data obtained from the SRIM are verified by comparing with standard data from the NIST PSTAR database.

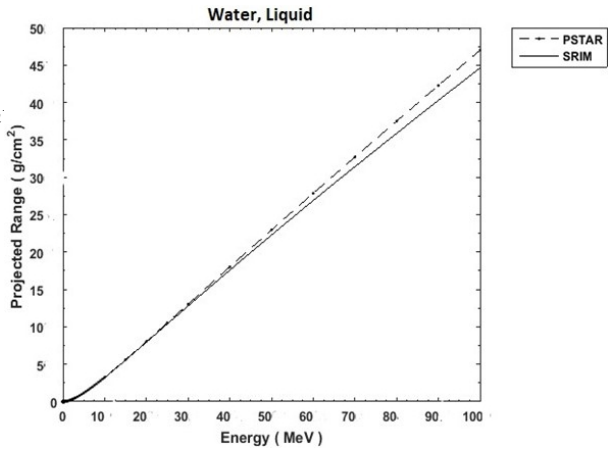

FIGURE 3. Projected range vs. energy graph shows the resemblance of SRIM data with PSTAR data at lower energies.

For the proton beam of low energy, there is quite a resemblance which is depicted in FIGURE 3.

Stopping Power and Range in Various Entrance Layers

When a proton beam impinges on the body, it transfers its energy to the body's various layers (shown in table 1). FIGURES 4. (a) and (b) illustrate the range vs. energy and stopping power vs. energy curves for the skin layer. It is found that the energy loss in this layer is negligible, and the stopping power for low-energy proton beams is exceptionally strong. Other layers, such as connective tissue, soft muscle, and the prostate gland, show a similar pattern, as shown in the FIGURES 4: c) and d) for connective tissue, e) and f) for soft muscle, and g) and h) for the prostate gland. When a high-energy proton collides with the body, this occurs.Therefore, to impart maximum energy to the prostate gland the proton beam should have minimum energy.Furthermore, it is proved that nuclear contact has a negligible effect on total stopping power. The electrical interaction of protons accounts for the majority of energy loss. The reason for this is that the proton is smaller than the target atoms and has a positive charge on it, which attracts the electron out of its orbit. Because high-energy particles have a high velocity, there is less time for interaction, the stopping power appears to diminish as energy increases. The range vs. energy curve is similar for all layers, indicating that proton range in biological targets is a function of target density. FIGURE 5 depicts the large energy deposition caused by the ionization on the targeted tumor site and small amount of energy loss on several entrance layers (Skin, Connective tissue, Soft muscle and Prostate). The energy loss in electronic interaction i.e. ionization in various layers is given by the

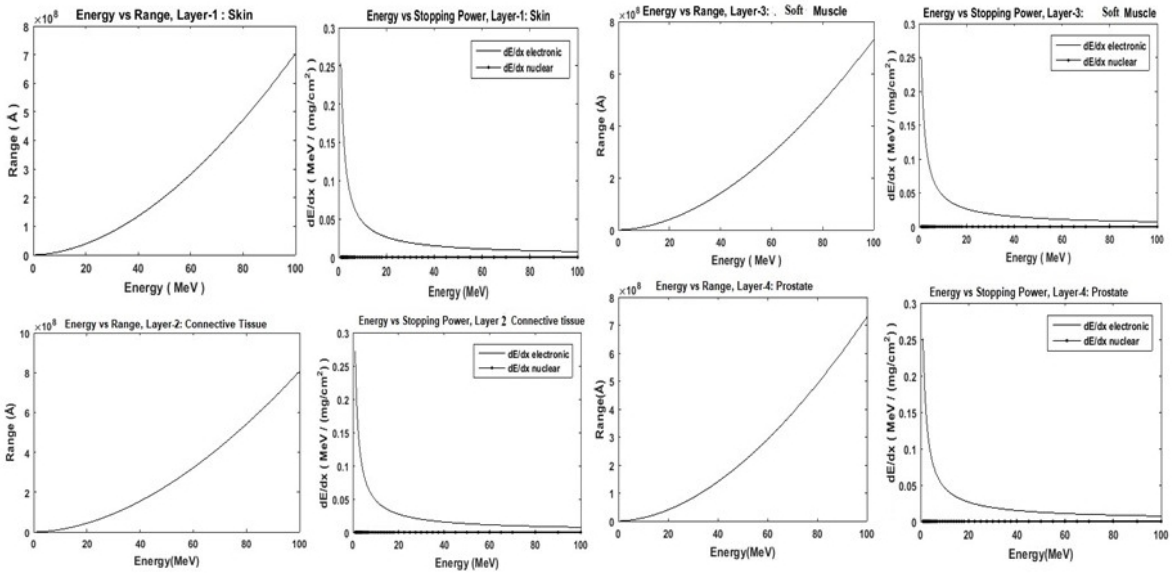

FIGURE 4. : a) Range Vs Energy for skin. b) Stopping power vs Energy for skin. c) Range Vs Energy for connective tissue. d) Stopping power vs Energy for connective tissue. e) Range Vs Energy for soft muscle. f) Stopping power vs Energy for soft muscle. g) Range Vs Energy for prostate. h) Stopping power vs Energy for prostate.

area under the graph. Energy deposited between the depth from 0 to 1.2 mm, which is mostly skin layer is 0.38388 MeV by ions and $6.52x10^{-5}$ MeV by recoils, between depth from 1.2 mm to 6.2 mm, which is mostly connective tissue is 6.5825 MeV by ions and $1.19x10^{-3}$ MeV by recoils, between depth from 6.2 mm to 11 mm ,which is mostly soft muscles equivalent layer is 14.649 MeV by ions and $2.66x10^{-3}$ MeV by recoils and between depth 11 mm to 31 mm, which is mostly Prostate is 42.877 MeV by ions and $8.79x10^{-3}$ MeV by recoils, beyond Prostate no energy loss is seen due to ionization by ion and recoils. The Bragg peak is seen at 33 mm, this implies that the energy deposition is maximum at targeted site i.e. at the end of the range and the ionization by recoil is negligible. A little irregularity is seen in the graph at connective tissue layer. As the protons move through the body it slows down, causing increased interaction with orbiting electrons. As expectation, the maximum proton deposition is on the target cells which is demonstrated by a peak i.e. Bragg peak, in FIGURE 5. The surrounding healthy cells receive significantly less injury than the cells in the designated volume and the healthy cells beyond target remains unaffected. Ionization by recoiling atom is less than that of proton itself, because of the larger size of recoil atom and lack of charge on it. The discrepancy in the graph at connective layer is explained by relatively lower concentration of heavy element like Na, Mg, P, Cl, etc.

Energy Loss due to Phonon

Phonons are created on nuclear interaction i.e. when energized proton or recoil atom interacts with the target atom causing them to vibrate. The total energy loss due to phonons consists of the direct creation of phonons by the ion, and the additional energy loss by target recoil atoms to phonons. The plot of energy loss on phonon by ions and recoils vs. target depth is shown in FIGURE 6. It revels that the phonon is mainly produced due to the recoil than ions itself. The energy loss due to the phonon is negligible in comparison to energy loss due to ionization. The total energy loss due to the phonon is $3.31x10^{-3}$ MeV by ions and $1.05x10^{-2}$ MeV due to the recoils. When proton travels through the human body it mainly interacts with orbital electron of the atoms due to its small size and charge on it. However, recoiling atoms have comparable size to target atoms and are thus responsible for production of maximum phonon.

Ion Range

The final distribution of photon beam of energy 65 MeV used to irradiate the Prostate tumor is depicted in FIGURE 6. It illustrates that the final distribution of the proton is maximum at the end of its range which explains occurrence of Bragg peak. The stopping power or linear energy transport of proton is inversely proportional to its velocity. The fast moving proton slows down as it tra-

verses the tissues by mostly the electronic interaction and eventually the maximum interaction occurs at the end of the range i.e. the expected target area. The ion statistics section of TRIM calculation is presented below: Proton average range = 340800000 Å Straggling = 4599000 Å Proton lateral range = 4752000 Å Straggling = 6992000 Å Proton radial range = 7487000 Å Straggling = 6456000 Å Comparing the average range with projected range from SRIM the error in calculation is 3.04

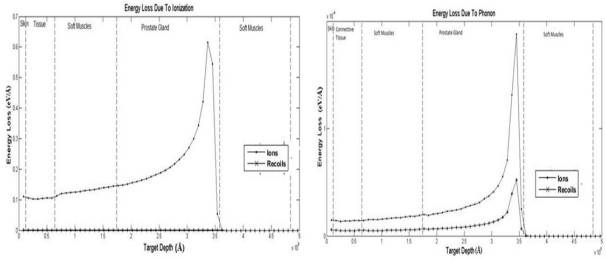

FIGURE 5. Projected range vs. energy graph shows the resemblance of SRIM data with PSTAR data at lower energies.

Lateral Distribution

FIGURE 7 summarizes the lateral and radial spread of ions within the target window. The lateral projected range is defined as the average of the absolute values of the projected displacements from the x-axis whereas, the radial range is the mean radial displacements range from the x-axis assuming cylindrical symmetry. As seen on the graph the lateral distribution of proton is fluctuating from 0 to 21 mm. Majority of protons are concentrated on prostate region. This allows oncologist shaping of dose to be delivered on accordance with the shape of the tumor.

CONCLUSION

From the above result, it is concluded that proton beam therapy is one of the best radiation therapy techniques for the treatment of prostate cancer cells. After finding the depth of the prostate tumor from the skin layer, the energy for proton beam is determined for biological medium by using stopping and range table for phantom. This shows the trustworthy of SRIM software for this kind of research and for treatment planning. TRIM data shows that 99.96% of the energy of proton is lost in the process of ionization by ion and 0.02% in ionization by recoils and only 0.01% energy is lost by production of phonon by ion and 0.02% by recoils. 65 MeV of the energy deposited on various layers viz. skin, connective tissue, soft muscles and prostate are approximately 0.384 MeV (i.e. 0.595%), 6.585 MeV (i.e. 10.20%), 14.654 MeV (22.71%), and 42.896 MeV (66.49%) respectively with the calculation error 0.74%. This concludes that proton beam therapy can damage the cancerous cell effectively without harming the surrounding healthy tissue. This ensures that there is negligible side effect for the proton beam therapy which is more in the conventional radiological treatment. Therefore, besides prostate cancer, proton beam therapy is particularly effective for treating irregular shaped tumors, hard to reach tumor, tumor near vital

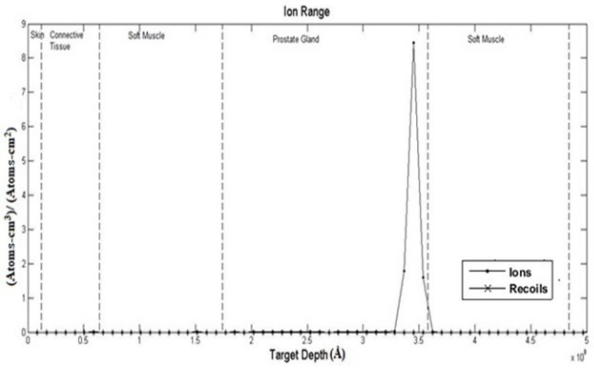

FIGURE 6. Projected range vs. energy graph shows the resemblance of SRIM data with PSTAR data at lower energies.

organs and critical structures and localized tumors that have not spread to other areas.This concludes that proton beam therapy damages the cancerous cell effectively and does not harm the other healthy tissues in the body. It infers that side effect after the proton beam therapy is less than any other radiological treatments.Therefore, proton beam therapy is particularly effective for treating irregular shaped tumors, hard to reach tumor, tumor near vital organs and critical structures and localized tumors that have not spread to other areas.

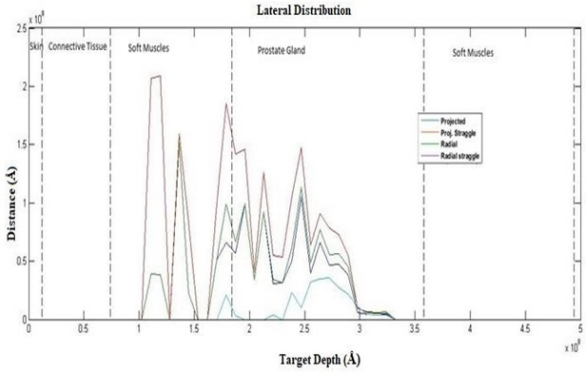

FIGURE 7. Lateral range distribution plot.

REFERENCES

1. H. Liu and J. Y. Chang, "Proton therapy in clinical practice," Chinese journal of cancer **30**, 315 (2011).
2. X. Tian, K. Liu, Y. Hou, J. Cheng, and J. Zhang, "The evolution of proton beam therapy: Current and future status," Molecular and clinical oncology **8**, 15–21 (2018).
3. K. Giri, B. Paudel, and B. Gautam, "Calculation of energy loss of proton beam on thyroid tumor," Himalayan Physics , 80–85 (2020).
4. B. Rosenzweig, N. M. Hoffmann, L. Lacombe, and N. T. Maitra, "Analysis of the classical trajectory treatment of photon dynamics for polaritonic phenomena," The Journal of Chemical Physics **156**, 054101 (2022).
5. C. Tobias, J. Lawrence, J. Born, R. McCombs, J. Roberts, H. Anger, B. Low-Beer, and C. Huggins, "Pituitary irradiation with high-energy proton beams a preliminary report," Cancer research **18**, 121–134 (1958).
6. E. Bass, A. Pantovic, M. Connor, R. Gabe, A. Padhani, A. Rockall, H. Sokhi, H. Tam, M. Winkler, and H. Ahmed, "A systematic review and meta-analysis of the diagnostic accuracy of biparametric prostate mri for prostate cancer in men at risk," Prostate Cancer and Prostatic Diseases **24**, 596–611 (2021).
7. M. Takagi, Y. Demizu, O. Fujii, K. Terashima, Y. Niwa, T. Daimon, S. Tokumaru, N. Fuwa, M. Hareyama, and T. Okimoto, "Proton therapy for localized prostate cancer: long-term results from a single-center experience," International Journal of Radiation Oncology* Biology* Physics **109**, 964–974 (2021).
8. M. S. Elmahdy, T. Jagt, R. T. Zinkstok, Y. Qiao, R. Shahzad, H. Sokooti, S. Yousefi, L. Incrocci, C. Marijnen, M. Hoogeman, *et al.*, "Robust contour propagation using deep learning and image registration for online adaptive proton therapy of prostate cancer," Medical physics **46**, 3329–3343 (2019).
9. M. J. Berger, "Estar, pstar, and astar: Computer programs for calculating stopping-power and range tables for electrons, protons, and helium ions," Unknown (1992).
10. A. Parisi, P. Olko, J. Swakoń, T. Horwacik, H. Jabłoński, L. Malinowski, T. Nowak, L. Struelens, and F. Vanhavere, "Microdosimetric characterization of a clinical proton therapy beam: comparison between simulated lineal energy distributions in spherical water targets and experimental measurements with a silicon detector," Physics in Medicine & Biology **67**, 015006 (2022).
11. O. Jäkel, "State of the art in hadron therapy," in *AIP Conference Proceedings*, Vol. 958 (American Institute of Physics, 2007) pp. 70–77.
12. K. Giri and R. Khanal, "Energy loss of proton beam on ovary tumor," Journal of Nepal Physical Society **5**, 24–29 (2019).
13. J. Y. Chang, X. Zhang, X. Wang, Y. Kang, B. Riley, S. Bilton, R. Mohan, R. Komaki, and J. D. Cox, "Significant reduction of normal tissue dose by proton radiotherapy compared with three-dimensional conformal or intensity-modulated radiation therapy in stage i or stage iii non–small-cell lung cancer," International Journal of Radiation Oncology* Biology* Physics **65**, 1087–1096 (2006).
14. M. Yoon, S. H. Ahn, J. Kim, D. H. Shin, S. Y. Park, S. B. Lee, K. H. Shin, and K. H. Cho, "Radiation-induced cancers from modern radiotherapy techniques: intensity-modulated radiotherapy versus proton therapy," International Journal of Radiation Oncology* Biology* Physics **77**, 1477–1485 (2010).
15. B. Schaffner and E. Pedroni, "The precision of proton range calculations in proton radiotherapy treatment planning: experimental verification of the relation between ct-hu and proton stopping power," Physics in Medicine & Biology **43**, 1579 (1998).
16. M. Yang, X. R. Zhu, P. C. Park, U. Titt, R. Mohan, G. Virshup, J. E. Clayton, and L. Dong, "Comprehensive analysis of proton range uncertainties related to patient stopping-power-ratio estimation using the stoichiometric calibration," Physics in Medicine & Biology **57**, 4095 (2012).
17. K. Giri and A. Bhandari, "Computational study of damage profiles and energy loss of gallium ion in germanium substrate," Journal of Nepal Physical Society **6**, 117–122 (2020).
18. K. Giri and B. Kandel, "Study of damage profiles and energy calculation of arsenic ions during ion implantation on germanium," BIBECHANA **17**, 96–103 (2020).
19. D. Jette and W. Chen, "Creating a spread-out bragg peak in proton beams," Physics in Medicine & Biology **56**, N131 (2011).
20. W. D. Newhauser and R. Zhang, "The physics of proton therapy," Physics in Medicine & Biology **60**, R155 (2015).